



# Journal of Applied Sciences

ISSN 1812-5654

**science**  
alert

**ANSI***net*  
an open access publisher  
<http://ansinet.com>

## Dynamic Rigidity Analysis of High-Speed Angular Contact Ball Bearing

Zhang Gang, Xu Quan, Zhi Han-Li, Jiang Xiao-Ying and Ni Xiao-Ting  
 Research Institute of Bearing, School of Mechanical and Electronic Engineering and Automation,  
 Shanghai University, Shanghai 200072, China

**Abstract:** At high rotational speed operating condition, there is much significance to analyze the bearing's dynamic rigidity, especially when the supporting precision is required. Based on classic analysis methods and essential theories of ball bearing, including Hertz contact theory and raceway control theory, develop a solving procedure to analyze the dynamic rigidity of high-speed angular contact ball bearing, according New-Raphson method. This procedure is greatly simplified and easy to be realized by program, since the correlations of the variables are founded. Selecting HP7005CTA under the fixed-pressure preload, used in high-speed motorized spindle as an example, we calculate the contact deformation, stress and angle between ball and raceway, then conclude the bearing's dynamic rigidity. The results show the effects of axial preload, rotational speed, inner and outer raceway curvature on bearing's axial, radial and angular rigidity.

**Key words:** High-speed angular contact ball bearing, fixed-pressure preload, dynamic rigidity, raceway curvature

### INTRODUCTION

Angular contact ball bearings play an important role in supporting the high-speed precision motorized spindle used for grinding machine. The bearing's dynamic rigidity determines the supporting performance, grinding precision and lifetime. Besides, higher dynamic rigidity has positive influence in reducing the vibration and noise (Harris, 2007; Jones, 1959; Foord, 2006).

Based on calculation of contact stress, angle and rigidity between ball and raceway, this paper analyzes the dynamic rigidity of high-speed angular contact ball bearing under fixed-pressure preload. More energy is expended in programming and analyzing the effects of various preload, rotational speed and raceway curvature on bearing's dynamic rigidity. The final conclusion has theory meaning to increase bearings' dynamic rigidity and optimization of motorized spindle.

### ESSENTIAL THEORIES

**Static analysis of bearing:** Under fixed-pressure preload  $F_0$ , bearing's contact angle and stress will be changed, comparing the situation of initial zero preload.

$\delta_a^0$  is the distance between the center of inner and outer rings.  $\alpha$  is the contact angle, while  $\alpha^0$  represents the initial contact angle.

The relations of these values are as below (Harris, 2007):

$$\frac{F_0}{ZD^2K} = \sin \alpha \left( \frac{\cos \alpha^0}{\cos \alpha} - 1 \right)^{1.5} \quad (1)$$

$$\delta_a^0 = \frac{A \sin(\alpha - \alpha_0)}{\cos \alpha} \quad (2)$$

where, Z means the number of balls, Dw is the diameter of ball, K is a constant. Newton-Raphson method can be used to calculate the equation (1) and get the value of  $\alpha$ . As the basis of dynamic analysis, the results of static analysis are referred to be initial iteration values of bearing's dynamic analysis.

**Hertz contact rigidity and bearing's rigidity:** According to Hertz contact theory, the contact rigidities between ball and raceways are:

$$K_{ij} = 1.5 \left[ \frac{\pi E'}{3 \Gamma_{ij} k_{ij}} \right]^{2/3} \left[ \frac{2e_{ij}}{\Gamma_{ij} \sum \rho_{ij}} \right]^{1/3} Q_{ij}^{1/3} \quad (3)$$

$$K_{oj} = 1.5 \left[ \frac{\pi E'}{3 \Gamma_{oj} k_{oj}} \right]^{2/3} \left[ \frac{2e_{oj}}{\Gamma_{oj} \sum \rho_{oj}} \right]^{1/3} Q_{oj}^{1/3} \quad (4)$$

where, i, o stand for inner and outer contact separately. Q means the contact stress between two bodies.

In the Figure 1,  $\alpha_{ij}$  and  $\alpha_{oj}$  are the dynamic contact angles between ball and raceways. Axial and radial components of contact rigidities are:

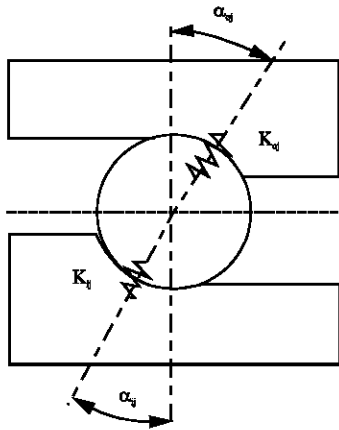


Fig. 1: Contact rigidities of ball and raceways

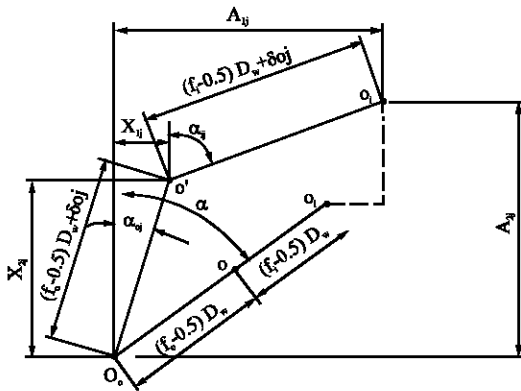


Fig. 2: Geometric deformation of bearing's elements at working condition

$$\begin{aligned} K_{aij} &= K_{ij} \sin^2 \alpha_{ij}, K_{aoj} = K_{oj} \sin^2 \alpha_{oj} \\ K_{rij} &= K_{ij} \cos^2 \alpha_{ij}, K_{roj} = K_{oj} \cos^2 \alpha_{oj} \end{aligned} \quad (5)$$

$K_a$ ,  $K_r$  and  $K_\theta$  are separately the axial, radial and angular dynamic rigidity of angular contact ball bearing. According to Fig. 1, the following equations can be obtained:

$$K_a = \sum_{j=1}^z \frac{K_{aij} K_{aoj}}{K_{aij} + K_{aoj}} \quad (6)$$

$$K_r = \sum_{j=1}^z \frac{K_{rij} K_{roj}}{K_{rij} + K_{roj}} \cos^2 \frac{2\pi}{Z} (j-1) \quad (7)$$

$$K_\theta = d_m R_1 \sum_{j=1}^z \frac{K_{aij} K_{aoj}}{K_{aij} + K_{aoj}} \cos^2 \frac{2\pi}{Z} (j-1) \quad (8)$$

Through the equations above, it can be found the correlations between dynamic rigidity and contact angle

and stress. Next step, we will look for the method to calculate the contact angle and stress.

**Geometric deformation inside bearing:** With the change of working force loaded on bearing, both the contact angle and stress between ball and raceways will produce a corresponding variation. In the Fig. 2, the outer ring is assumed to be fixed.

$\delta_a$ ,  $\delta_r$  and  $\theta$  are the relative displacements of inner and outer ring in axial, radial and angular directions. As shown in Fig. 2:

$$A_{1j} = BD_w \sin \alpha + \delta_a + R_1 \theta \cos \psi_j \quad (9)$$

$$A_{2j} = BD_w \cos \alpha + \delta_r \cos \psi_j \quad (10)$$

where,  $R_1$  is the distance from center of inner ring to bearing center of curvature.  $R_1 = d_m / 2 + (f_1 - 0.5) D_w \cos \alpha$ .

Besides, the following equations can be obtained (Harris, 2007; Chen *et al.*, 2012):

$$X_{1j}^2 + X_{2j}^2 = [(f_0 - 0.5) D_w + \delta_{oj}]^2 \quad (11)$$

$$(A_{1j} - X_{1j})^2 + (A_{2j} - X_{2j})^2 = [(f_1 - 0.5) D_w + \delta_{ij}]^2 \quad (12)$$

**FORCE ANALYSIS**

Based on quasi-static analysis of roller bearing and outer raceway control theory, it can be obtained that  $\lambda_{ij} = 0$ ,  $\lambda_{oj} = 0$  (Harris, 2007):

As shown in Fig. 3, the following equations can be obtained:

$$Q_{ij} \sin \alpha_{ij} - Q_{oj} \sin \alpha_{oj} + 2 \frac{M_{\theta j}}{D_w} \cos \alpha_{oj} = 0 \quad (13)$$

$$Q_{ij} \cos \alpha_{ij} - Q_{oj} \cos \alpha_{oj} - 2 \frac{M_{\theta j}}{D_w} \sin \alpha_{oj} + F_{cj} = 0 \quad (14)$$

where, Hertz contact stress between inner, outer ring and ball are expressed by  $Q_{ij} = K_{ij} \delta_{ij}^{3/2}$ ,  $Q_{oj} = K_{oj} \delta_{oj}^{3/2}$ .

$K_{ij}$  and  $K_{oj}$  are the constant curvatures of stress-deformation and can be calculated by literature reference (Harris, 2007; Panda and Dutt, 2003).

Considering the axial and radial balance of inner ring under load, the following equations can be obtained:

$$F_a - \sum_{j=1}^{j=z} Q_{ij} \sin \alpha_{ij} = 0 \quad (15)$$

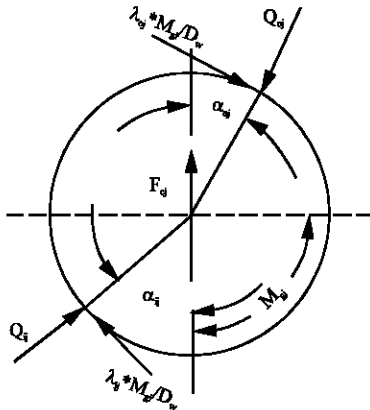


Fig. 3: Forces and moments acting on a ball

$$F_r - \sum_{j=1}^{j=Z} Q_{ij} \sin \alpha_{ij} = 0 \quad (16)$$

$$M - \sum_{j=1}^{j=Z} Q_{ij} \sin \alpha_{ij} R_1 \cos \psi_{ij} = 0 \quad (17)$$

where,  $F_a$ ,  $F_r$  and  $M$  means the axial, radial and moment loads on angular contact ball bearing.

We can find the values of  $\cos \alpha_{ij}$ ,  $\sin \alpha_{ij}$ ,  $\cos \alpha_{ij}$ ,  $\sin \alpha_{ij}$ ,  $Q_{ij}$  and  $Q_{oj}$ . The following Eq. 18-22 can be obtained from 13-17:

$$\frac{\lambda_{0j} M_{0j} X_{2j} / D_w - K_{0j} \delta_{0j}^{1.5} X_{1j} + K_{1j} \delta_{1j}^{1.5} (A_{1j} - X_{1j})}{(f_0 - 0.5) D_w + \delta_{0j}} = 0 \quad (18)$$

$$\frac{\lambda_{zj} M_{zj} X_{1j} / D_w - K_{zj} \delta_{zj}^{1.5} X_{2j} - K_{2j} \delta_{2j}^{1.5} (A_{2j} - X_{2j})}{(f_0 - 0.5) D_w + \delta_{zj}} - F_{zj} = 0 \quad (19)$$

$$F_a - \sum_{j=1}^{j=Z} \frac{K_{1j} \delta_{1j}^{1.5} (A_{1j} - X_{1j})}{(f_1 - 0.5) D_w + \delta_{1j}} = 0 \quad (20)$$

$$F_r - \sum_{j=1}^{j=Z} \frac{K_{2j} \delta_{2j}^{1.5} (A_{2j} - X_{2j})}{(f_1 - 0.5) D_w + \delta_{2j}} = 0 \quad (21)$$

$$M - \sum_{j=1}^{j=Z} \frac{K_{1j} \delta_{1j}^{1.5} (A_{1j} - X_{1j})}{(f_1 - 0.5) D_w + \delta_{1j}} R_1 \cos \psi_j = 0 \quad (22)$$

### SOLVING PROCEDURE OF DYNAMIC RIGIDITY CALCULATION

The Eq. 11, 12 and 18-22 are the basis to analyze bearing's dynamic performance. Because  $j$  varies from 1 to  $Z$ , there are  $(4Z+3)$  equations from which  $X_{1j}$ ,  $X_{2j}$ ,  $\delta_{1j}$ ,  $\delta_{2j}$ ,  $\delta_w$ ,  $\delta$ , and  $\theta$  can be calculated by Newton-Raphson method.

Furthermore, we found that  $X_{1j}$ ,  $X_{2j}$ ,  $\delta_{1j}$  and  $\delta_{2j}$  are actually the functions of contact angles  $\alpha_{ij}$  and  $\alpha_{oj}$  as shown in the equations below:

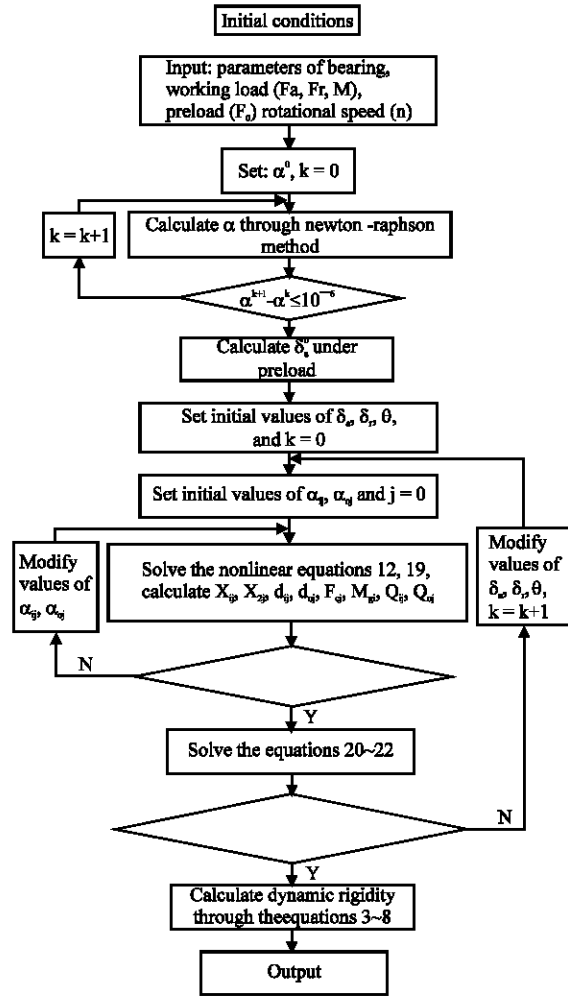


Fig. 4: Solving procedure of bearing's dynamic rigidity

$$X_{1j} = \frac{A_{2j} \tan \alpha_{ij} - A_{1j} \tan \alpha_{oj}}{\tan \alpha_{ij} - \tan \alpha_{oj}} \quad (23)$$

$$X_{2j} = \frac{A_{2j} \tan \alpha_{ij} - A_{1j}}{\tan \alpha_{ij} - \tan \alpha_{oj}} \quad (24)$$

$$\delta_{ij} = \frac{A_{1j} \cos \alpha_{oj} - A_{2j} \sin \alpha_{oj}}{\sin(\alpha_{ij} - \alpha_{oj})} - (f_1 - 0.5) D_w \quad (25)$$

$$\delta_{oj} = \frac{A_{2j} \sin \alpha_{ij} - A_{1j} \cos \alpha_{ij}}{\sin(\alpha_{ij} - \alpha_{oj})} - (f_0 - 0.5) D_w \quad (26)$$

$M_{0j}$  and  $F_{zj}$  can also be expressed by contact angles  $\alpha_{ij}$  and  $\alpha_{oj}$ . Since these correlations are founded, the solve procedure of nonlinear equations will be simplified greatly. The flow chart of solving bearing's dynamic rigidity is shown in Fig. 4.

**RESULTS AND ANALYSIS OF DYNAMIC RIGIDITY**

According to the solving procedure above, we select the high-speed precision angular contact ball bearing HP7005CTA as an object to calculate, then explore its

dynamic rigidity. The parameters of bearing HP7005CTA are listed in Table 1. The dynamic rigidity values obtained through the simulation are shown in Fig. 5-16.

**Effect of preload on dynamic rigidity:** The effect of preload variation on dynamic rigidity is investigated,

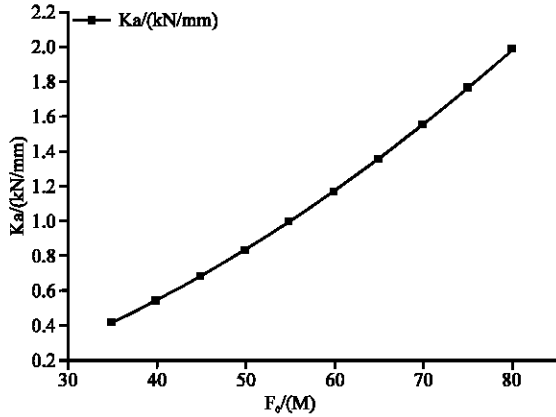


Fig. 5: Axial rigidity under various preload

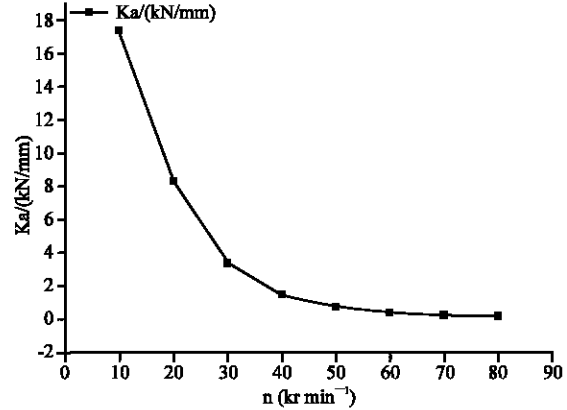


Fig. 8: Axial rigidity at various rotational speed

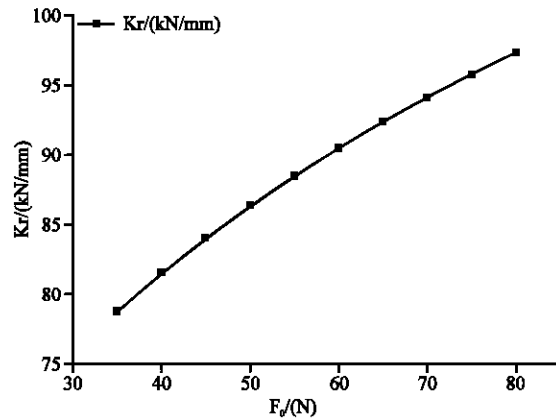


Fig. 6: Radial rigidity under various preload

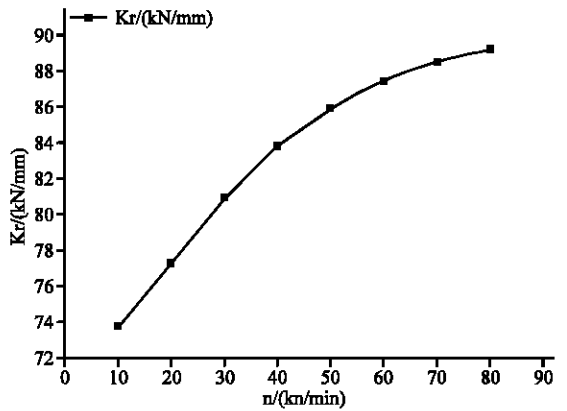


Fig. 9: Radial rigidity at various rotational speed

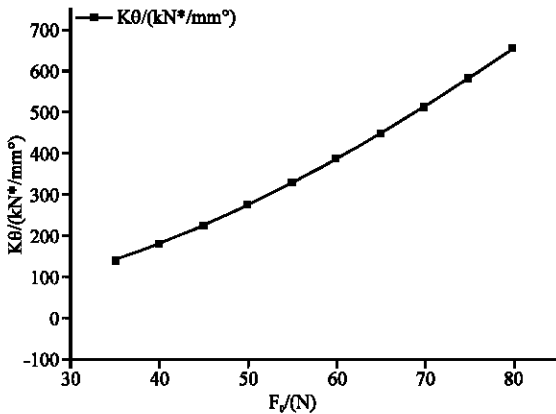


Fig. 7: Angular rigidity under various preload

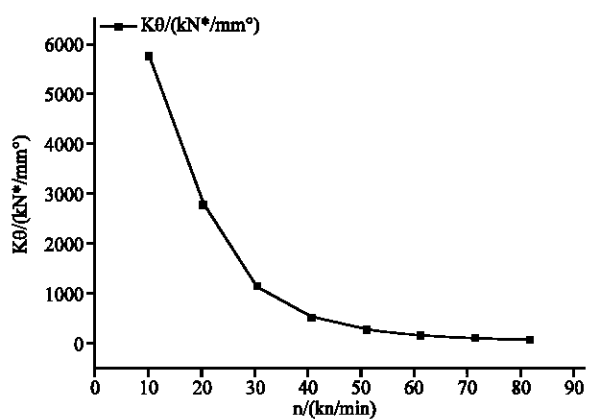


Fig. 10: Angular rigidity at various rotational speed

Table 1: Parameters of bearing HP7005CTA

Parameter	Value
Inside diameter of bearing $d/mm$	25
Outside diameter of bearing $D/mm$	47
Width of bearing $B/mm$	12
Diameter of ball $D_w/mm$	5.556
Contact angle $\alpha/^\circ$	15
Number of balls $Z$	15
Elastic modulus $E/GPa$	206
Poisson's ratio $\nu$	0.3
Density $\rho / kg\cdot m^{-3}$	$7.8 \times 10^3$

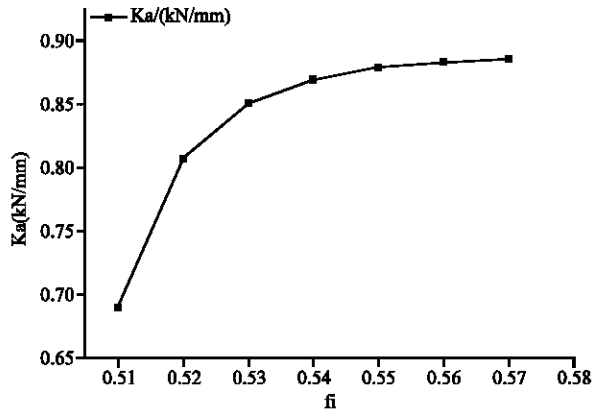


Fig. 11: Axial rigidity for various inner curvature

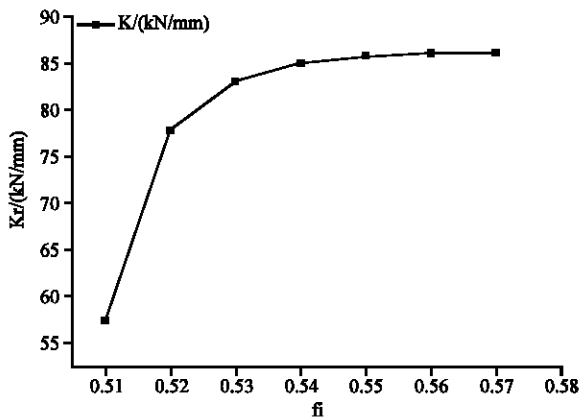


Fig. 12: Radial rigidity for various inner curvature

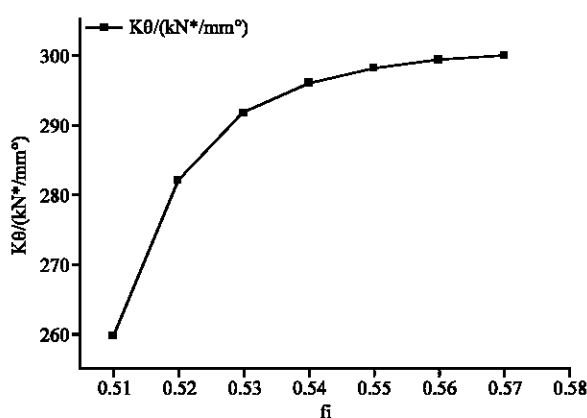


Fig. 13: Angular rigidity for various inner curvature

when the inner ring rotational speed is  $48000 \text{ r} \cdot \text{mm}^{-1}$ . From Fig. 5-7, we can conclude that bearing's axial, radial and angular rigidities are increased with the rise of axial preload. The reason is there will be bigger contact angles and stress between ball and raceways, when the preload pressure is larger.

**Effect of rotational speed on dynamic rigidity:** Bearing's dynamic rigidities also vary with the rotational speed changes, as shown in Fig. 8-10.

As the rotational speed increase, radial rigidity is increased, while axial and angular rigidity are decreased. This is because the increasing centrifugal force reduces the outer contact angle  $\alpha_{oj}$ , while the inner contact angle  $\alpha_{ij}$  is increased and the outer contact rigidity  $K_{oj}$  is increased, the inner contact rigidity  $K_{ij}$  is decreased.

**Effect of inner and outer raceway curvatures on dynamic rigidity:** Fig. 11-16 show the correlations between bearing's dynamic rigidity and raceway curvatures, at the rotational speed  $48000 \text{ r} \cdot \text{min}^{-1}$ .

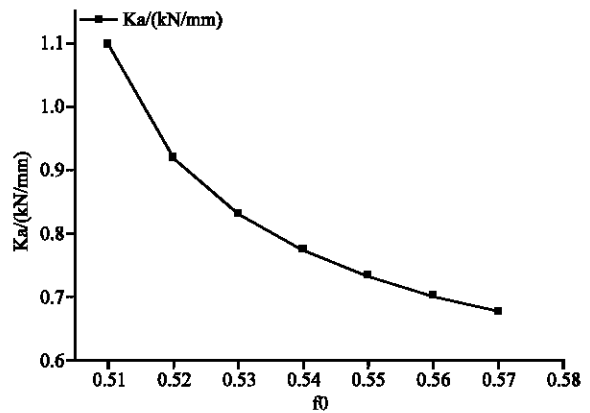


Fig. 14: Axial rigidity for various outer curvature

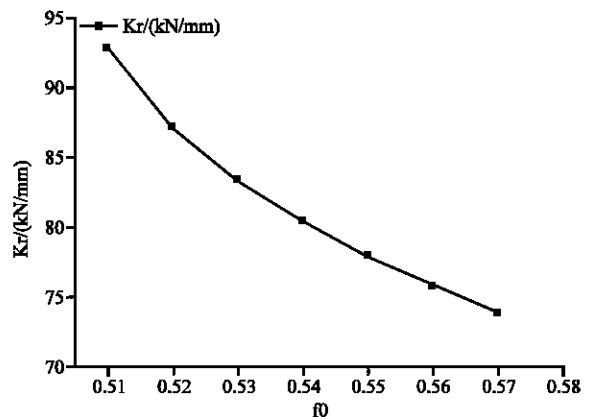


Fig. 15: Radial rigidity for various outer curvature

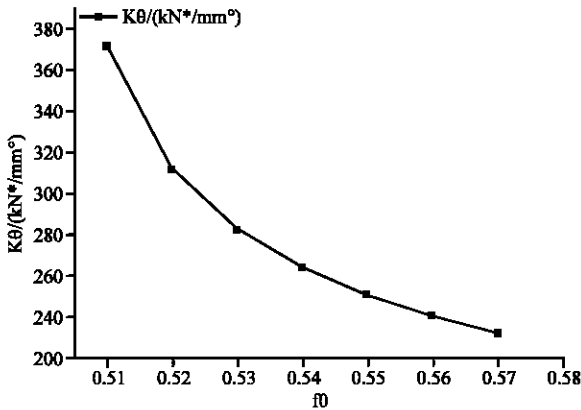


Fig. 16: Angular rigidity for various outer curvature

In Fig. 11-13, there is slowly rise of three rigidity curves when the inner raceway curvature is increased. But, according to Fig. 14-16, axial, radial and angular rigidities are decreased sharply with the increase of outer raceway curvature. Outer raceway curvature is an important factor to define bearing's dynamic rigidity. So, according the simulation results, we should take into account the outer raceway curvature, aiming at better high-speed angular contact ball bearing's dynamic rigidity.

### CONCLUSIONS

In this study, aiming at the better high-speed angular contact ball bearing's dynamic rigidity, we studied on classic analysis methods and developed an improved solving procedure. The dynamic rigidity was analyzed for various operating conditions and geometric parameters. The effects of various factors on dynamic rigidity are as follows:

- The larger preload pressure, the bigger axial, radial and angular rigidities of angular contact ball bearing
- Under fixed-pressure preload, radial rigidity is increased, while axial and angular rigidities are decreased at the higher rotational speed
- There is slowly rising of dynamic rigidity curves when the inner raceway curvature is increased. But, axial, radial and angular rigidities are decreased sharply with the increase of outer raceway curvature

### ACKNOWLEDGMENT

Supported by 2012 Shanghai Alliance Plan: Technology of Temperature Control of High-speed Precision Motorized Spindle (No. LM201250).

### REFERENCES

- Chen, W., Z. Ma, L. Gao, X. Li and J. Pan, 2012. Quasi-static analysis of thrust-loaded angular contact ball bearings part I: theoretical formulation. *Chin. J. Mech. Eng.*, 25: 71-80.
- Foord, C.A., 2006. High-speed ball bearing analysis. *Proc. Inst. Mech. Eng. Part G: J. Aerosp. Eng.*, 220: 537-544.
- Harris, T.A., 2007. *Rolling Bearing Analysis: Advanced Concepts of Bearing Technology*. 5th Edn., Taylor and Francis, New York.
- Jones, A.B., 1959. Ball motion and sliding friction in ball bearings. *J. Basic Eng.*, 81: 1-12.
- Panda, K.C. and J. K. Dutt, 2003. Optimum support characteristics for rotor-shaft system with preloaded rolling element bearings. *J. Sound Vibr.*, 260: 731-755.